Int. J. Environ. Sci. Technol. (2015) 12:1261–1268
DOI 10.1007/s13762-013-0473-z

ORIGINAL PAPER

Impacts of load mass on real-world PM_1 mass and number emissions from a heavy-duty diesel bus

C. Wang · Y. Wu · J. Jiang · S. Zhang · Z. Li · X. Zheng · J. Hao

Received: 24 June 2013 / Revised: 2 November 2013 / Accepted: 2 December 2013 / Published online: 8 January 2014

Abstract On-road emission profiles of ultra-fine particle matter with aerodynamic diameter <1 μm (PM_1) were obtained from a Euro IV diesel bus in Beijing under two typical load mass conditions. PM_1 mass and number emissions were recorded second by second using an electrical low-pressure impactor (ELPI). An on-road driving mode binning method was applied to relate instantaneous emission rate with real-time on-road driving conditions, and an engine-operating mode binning method was used to explore the impacts of engine load on PM_1 emission characteristics. Our results show that higher load mass will increase both particle mass and number emissions. Measured PM_1 mass emission factors were 0.147 and 0.185 g/km under low and high load mass conditions, respectively. PM_1 number emission factors were 3.71×10^{13} and 4.58×10^{13} #/km. In addition, load mass also influenced the size-resolved concentration of PM mass and number from that sampled bus. For example, under low load mass conditions, an obvious peak of PM number concentration was observed situated in the second channel of the ELPI corresponding to the median diameter 63 nm. By contrast, peak concentration of the PM number was increased under high load mass conditions and situated in the third channel of the ELPI corresponding to the median diameter 109 nm.

Keywords PM_1 · Particle number · Diesel bus · Size distribution · Engine load

C. Wang · Y. Wu (✉) · J. Jiang · S. Zhang · Z. Li · X. Zheng · J. Hao
School of Environment, and State Key Joint Laboratory of Environment Simulation and Pollution Control, Tsinghua University, Beijing 100084, China
e-mail: ywu@tsinghua.edu.cn

C. Wang
Research Institute of Chemical Defence, Beijing 102205, China

Y. Wu · J. Jiang · J. Hao
State Environmental Protection Key Laboratory of Sources and Control of Air Pollution Complex, Beijing 100084, China

Introduction

In China, an impressive growth in total vehicle population has been accompanied by rapid economic and social development since the 1990s (Wu et al. 2012a). Vehicle emissions are identified as one of the most important sources of urban air pollution (Kho et al. 2007; Malakootian and Yaghmaeian 2004), especially in some megacities such as Beijing and Guangzhou (Du et al. 2012; Hao et al. 2001; Zhang et al. 2013; Zhou et al. 2010). China's government has been making great efforts to control vehicle emissions in order to improve urban air quality (Wu et al. 2011). Among all vehicle categories, heavy-duty diesel vehicles (HDDVs) receive special attention due to their substantially higher emission factors of nitrogen oxides (NO_X) and particle matters (PM) (Wu et al. 2012b), relative to those of light-duty gasoline vehicles (Wang et al. 2013). In particular, diesel PM is identified as one of the mobile source air toxics and has become a major source of environmental pollution, especially in urban areas (Giechaskiel et al. 2012; Maricq 2007; Song et al. 2012, 2013; Wu et al. 2014). Furthermore, a working group of the International Agency for Research on Cancer (IARC) recently assessed the carcinogenicity of gasoline and diesel engine exhaust in June 2012 (Benbrahim-Tallaa et al. 2012). The most significant outcome of that evaluation was the upgrade classification of diesel exhaust, from Group 2A "probably carcinogenic to human" to Group 1 "carcinogenic to human" with sufficient evidence for lung

cancer (Benbrahim-Tallaa et al. 2012; Scheepers and Vermeulen 2012). Epidemiological studies have demonstrated that smaller diameter PM can reach the lower human airways and lead to adverse health effects (Oberdorster et al. 2004; Somers et al. 2004). Furthermore, submicron fractions of PM with aerodynamic diameter <1 μm (PM_1), which are the dominant part of diesel PM number emissions, have significantly stronger physiological effects than larger diameter PM (Mazzarella et al. 2012; Pope 2000).

To mitigate diesel particulate emissions, increasingly stringent emission standards are implemented for new HDDVs. For example, the regulatory emission limits for particle mass of the Euro IV standard have become substantially tightened compared to those of the Euro III standard, from 0.10 to 0.02 g/kW h under the steady test cycle (i.e., the European Steady Cycle, ESC) and from 0.16 to 0.03 g/kW h under the transient test cycle (i.e., the European Transient Cycle, ETC) (Giechaskiel et al. 2012; Wu et al. 2012b). The Euro V standard for HDDVs remains at the same stringent level for particle mass emissions as that of the Euro IV standard. In China, however, those more stringent emission standards (e.g., Euro IV and Euro V) have been currently adopted only by the public fleets (e.g., urban public buses) in megacities, such as Beijing and Shanghai (Zhang et al. 2014). The Euro VI emission standard introduces regulatory limits for particle number emissions in addition to tightened limits for particle mass emissions, which would bring a renewed focus on particle number emissions from HDDVs (Giechaskiel et al. 2012).

Impacts of operating conditions on PM emission characteristics (e.g., particle mass, particle number, and size distribution) have been reported in previous studies based on laboratory measurements using a dynamometer. For example, Lähde et al. (2011) identified an increasing trend of PM emissions in the nonvolatile nucleation mode (i.e., the core mode) at medium and high load conditions in dynamometer testing. Ushakov et al. (2013) found that engine load conditions had impacts on the size distribution. However, it should be noted that those test conditions do not represent on-road driving conditions; when considering real-world driving speed, engine conditions, and load mass, there might be significantly different results with those fixed experimental conditions. Furthermore, on-road vehicular PM emissions could be tested by using on-board portable emission measurement systems (Liu et al. 2011; Wu et al. 2012b), on-road vehicle chasing (Tang and Wang 2006; Wang et al. 2011, 2012), remote sensing (Kuhns et al. 2004), and tunnel measurement (Grieshop et al. 2006). However, compared to the on-board PEMS, the other on-road measurement technologies mentioned above could only provide emission profiles for a rather short period without detailed record of instantaneous driving conditions for tested vehicles. Emission characteristics of PM_1 from HDDVs need to be further studied by using the on-board PEMS technology with potential impacts from on-road operating conditions taken into account.

In this paper, we measured on-road emission factors of particle mass and number from a Euro IV diesel bus under two typical load mass conditions. On-road driving and engine-operating mode binning methods are developed to relate emission rates with real-time operating conditions. In addition, we also explored the impacts of load mass on size distribution of particle mass and number concentration. This paper aims to provide a better understanding of PM emissions of HDDVs from an on-road perspective.

Materials and methods

Experimental section

One in-use heavy-duty diesel bus compliant with the Euro IV emission standards was tested in this study. The detailed information of the engine specifications is provided in Table 1. Figure 1 presents the schematic of the emission measurement system. The exhaust gas was diluted by a two-stage dilution tunnel setup. The dilution factor of each stage was maintained at approximately 8:1. Temperatures of those two dilution stages were controlled at about 150 and 30 °C, respectively. The dilution air was dried and pre-filtered. A Sensor Inc. SEMTECH-DS PEMS was used to measure on-road emissions of gaseous pollutants and to keep a record of instantaneous vehicle speed, engine conditions (e.g., engine speed and engine load), and fuel consumption rate (Wang et al. 2013; Wu et al. 2012b; Zhang et al. 2014). A Dekati electrical low-pressure impactor (ELPI) was used to measure real-time PM emission profiles including size-resolved concentration of particle mass and number second by second (Liu et al. 2011; Maricq et al. 2006). Furthermore, previous studies indicated that calculated particle mass on the basis of particle number concentration recorded by the ELPI could agree well with filter gravimetric measurement for conventional diesel vehicles (Maricq et al. 2006; Zervas et al. 2006). In this study,

Table 1 Engine specifications of the sampled bus

Parameter	Value
Engine model	Cummins ISBe4+ 225B
Model year	2007
Vehicle manufacturer	King Long
Emission standard	Euro IV
Rated torque at 1,500 RPM (Nm)	850
Number of cylinders	6
Engine displacement (L)	6.7
Accumulated mileage (km)	242,520

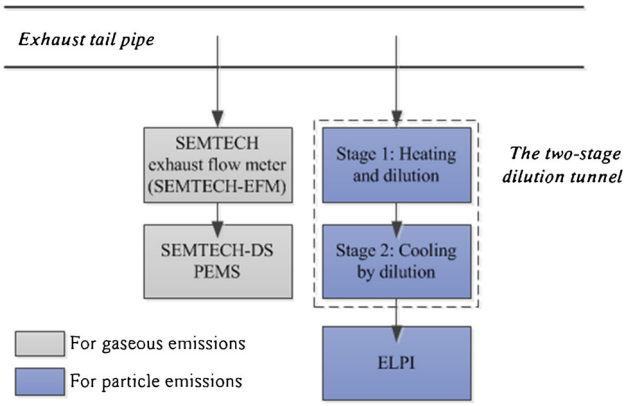

Fig. 1 Sketch of real-world vehicle emission measurement system installed in the tested bus

the first 8 ELPI channels (median diameters from 30 nm to 1.02 μm) are taken into account as the PM_1 fraction. All of the instruments were calibrated and tested individually with ambient air before carrying out the engine experiments.

A representative bus route in Beijing was chosen to simulate real operating conditions, which included frequent stops and starts. The tested bus was warmed up before each test. To evaluate the effects of load mass, this bus was tested under two states of load mass, respectively, such as high load mass (2.0 t) and low load mass (the total mass of measurement instrument, driver, and technicians is around 0.5 t). Low sulfur diesel fuel (with a sulfur content limit of 50 ppm) meeting the Euro IV diesel quality standard was used for the tested diesel bus during our study period.

On-road driving mode binning

In order to explore potential relationships between emission characteristics of diesel particulates and on-road driving conditions, a mode binning methodology is applied in this study. We use a proxy variable, vehicle-specific power (VSP), to indicate instantaneous vehicle power demand. VSP is defined as instantaneous power per unit mass of the vehicle and has been widely used in the development of vehicle emission models, such as the MOVES model by US Environmental Protection Agency (Koupal et al. 2004) and the EMBEV model by Tsinghua University (Wu et al. 2012b). Here, we calculated VSP by Eq. 1.

$$\text{VSP} = \frac{A}{m} \cdot v + \frac{B}{m} \cdot v^2 + \frac{C}{m} \cdot v^3 + av + gv \sin\theta \quad (1)$$

Where m is vehicle weight, tons; v is instantaneous vehicle speed, m/s; a is instantaneous vehicle acceleration, m/s^2; θ is road grade, radians; A is the rolling resistance coefficient, $kW \cdot s/m$; B is the rotational resistance coefficient, $kW \cdot s^2/m^2$; C is the aerodynamic drag coefficient, $kW \cdot s^3/m^3$. In this study, $\frac{A}{m}$, $\frac{B}{m}$, and $\frac{C}{m}$ are 0.0643 $kW \cdot s/m \cdot t$, 0 and 0.000279 $kW \cdot s^3/m^3 \cdot t$, respectively(Wu et al. 2012b).

A total of 22 on-road driving modes are eventually established, including a braking mode (i.e., bin 0), an idling mode (i.e., bin 1), and 20 modes presenting cruise or acceleration driving conditions (Wu et al. 2012b; Wang et al. 2013). Time allocations of each on-road driving mode are compared to test cycles under low and high load mass conditions and presented in Fig. 2, together with that for a typical driving cycle for urban buses in Beijing (i.e., BJBC) (Wu et al. 2012b). Because of frequent stops and driving congestion of urban buses, the average idling time share under low and high load mass conditions is 22 %, and low-speed zones with on-road driving mode bins 11–18 contribute approximately 60 % of total time for those two tested cycles. There are no data in the high-speed segment (i.e., bins 35–38) with speed over 80 km/h due to the city speed limit. As a result, average speeds of tested cycles under low and high load mass conditions are as low as 17.5 and 17.9 km/h, respectively. The average emission rates of particle mass and particle number of each on-road driving mode are estimated in a similar way as with emission rates of major air pollutants (Wu et al. 2012b). Furthermore, the distance-based emission factors of PM_1 mass and number are developed on the basis of average emission rate and time allocation of on-road driving mode bins with that typical driving cycle (i.e., BJBC).

Engine-operating mode binning

From the on-board diagnostic (OBD) system, we obtained detailed real-time data regarding engine-operating conditions, such as engine load and engine speed. They are key parameters which are highly related to engine emissions. As Fig. 3 indicates there is a reasonable linear correlation ($R^2 = 0.65$) between real-time engine load rate and calculated VSP.

We further constructed a total of six engine-operating modes with engine load rate and engine speed, illustrated in Table 2. Figure 4 presents an increasing trend in average VSP with engine-operating modes from BIN 01 to BIN 06, only with an exception of BIN 04. BIN 01 represents braking and deceleration driving modes. BIN 02 primarily represents the idling mode. BIN 03 represents transient driving conditions with mild acceleration and deceleration conditions. BINs 04–06 represent cruise and acceleration conditions with increasing engine power demand. For example, BIN 06 is an engine-operating mode with a high proportion of rapid accelerations, which are mainly made up of on-road driving modes bins 16–18 and bins 26–28 with average engine

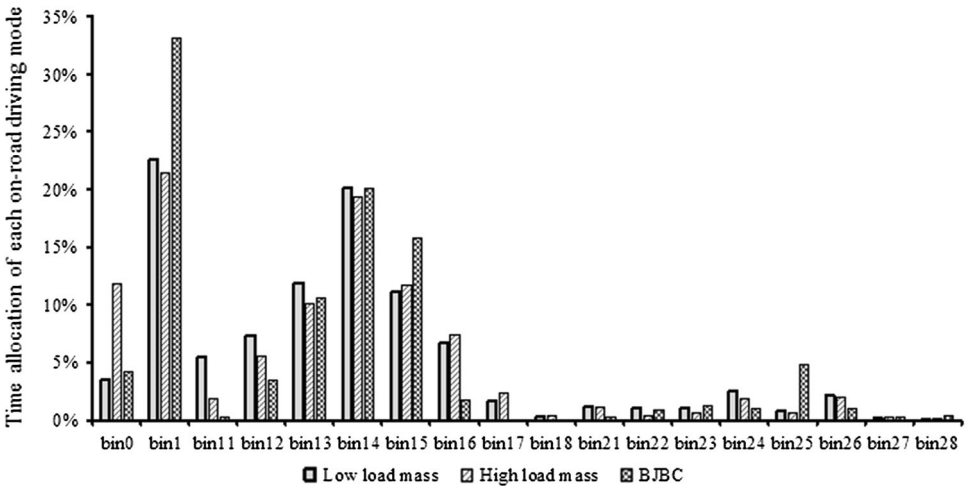

Fig. 2 Time allocation of each on-road driving mode bin to total time of tested cycles under low and high load mass conditions and a typical driving cycle for urban buses in Beijing

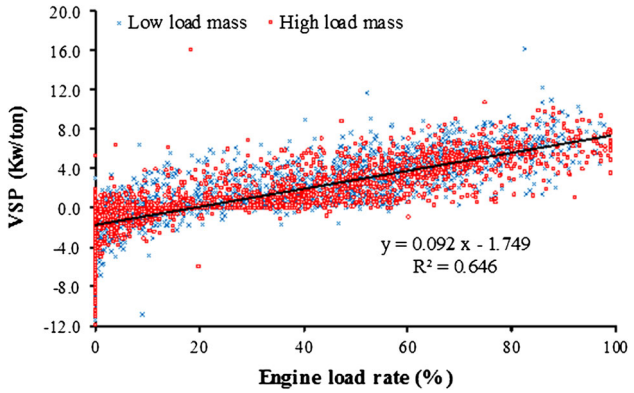

Fig. 3 Correlation between engine load rate and VSP

Table 2 Definition of engine-operating modes by using engine load rate and engine speed

Engine-operating mode	Engine load rate (%)	Engine speed (RPM)	Average engine load rate (%, Ave. ± SD)	
			Low load mass	High load mass
BIN 01	[0,5]	All	1.0 ± 1.7	0.6 ± 1.4
BIN 02	(5,30]	≦1,100	13.5 ± 5.3	13.8 ± 5.3
BIN 03	(5,30]	>1,100	17.1 ± 7.8	18.4 ± 7.3
BIN 04	(30,70]	≦1,100	38.3 ± 6.4	37.7 ± 6.6
BIN 05	(30,70]	>1,100	52.1 ± 10.8	51.2 ± 11.0
BIN 06	(70,100]	All	79.9 ± 7.0	81.8 ± 8.6

load rate approximately 80 % and average VSP over 5 kW/t. No statistically significant differences have been observed between low and high load mass conditions. However, it is worth noting that time allocation of BIN 06 (i.e., highest power demand mode) increased by 33 % (from 6.7 to 8.9 % to total time) when load mass was added which is the engine-operating condition mode with highest emission rates.

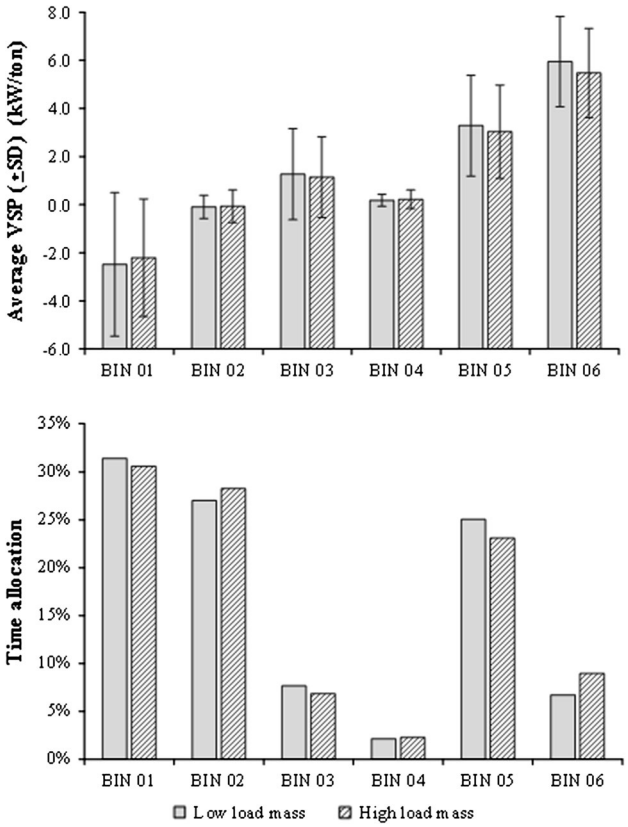

Fig. 4 Average VSP and time allocation of each engine-operating mode

Results and discussion

Emission factors of PM_1 mass and number

Emission factor of PM_1 mass was 0.147 g/km under the low load mass condition. It rose to 0.185 g/km when a load mass of 2 t was added, an increase of 26 %. In terms of the brake-specific emission factors, they are, respectively, 0.097 and 0.127 g/kW h under low and high load mass conditions, an

increase of 31 %. When compared to the Euro IV emission standard, they are both significantly higher than the regulatory limits of total exhaust PM mass. This is primarily attributed to the gap in engine-operating conditions between real-world driving cycle and regulatory test procedures (i.e., the ESC and the ETC) (Liu et al. 2011; Wu et al. 2012b). For example, Wu et al. (2012b) pointed out that 85 % of real-world operating time was beyond the ESC emission control zone for urban diesel buses in Beijing. Therefore, a specific testing cycle with more real-world driving features (e.g., low-speed stop-and-go driving conditions) for urban buses as well as an advanced in-use compliance testing program (e.g., the not-to-exceed (NTE) limits by using PEMS adopted by the US EPA) is necessary to control real-world PM emissions for urban buses in the future. Furthermore, decreasing trends in PM emission factors for both diesel buses and trucks with increasingly stringent emission standards (e.g., from Euro I to Euro V) have been identified from a large-sample on-road field study in Beijing (Wu et al. 2012b). Considering that HDDVs are a major contributor of PM emissions among all vehicle categories for many of China's megacities (e.g., Beijing, Guangzhou), the government should accelerate the implementation of tightened emission certifications for new HDDVs (e.g., Euro V and Euro VI) and phase out those older HDDVs with high emission factors (e.g., yellow-labeled vehicles). In addition, alternative fuel systems and advanced vehicle technologies (e.g., compressed natural gas, liquefied natural gas, hybrid electric, and battery electric) might play an important role in mitigating PM emissions for heavy-duty vehicles within the urban areas. This requires more measurement data to address in the future.

Figure 5 presents the average emission rates of PM_1 mass for each on-road driving mode bin under low and high load mass conditions, respectively. Average emission rates of bin 27–28 were ignored in this figure because of too few data available in those two modes (<10 s). Generally speaking, emission rates increase with VSP, which is similar to the trends for gaseous pollutants (e.g., CO, THC, and NO_X). Furthermore, the average PM_1 mass emission rates for those on-road driving modes with VSP higher than 0 kW/t (e.g., bin 14–18 and bin 24–26) are significantly increased under the high load mass condition, compared to those under low load mass condition. For example, PM_1 mass emission rates are higher by 19–73 % for bins 14–18 and 111–145 % for bins 24–26 under the high load mass condition relative to those under low load mass condition. To eliminate the distinction of driving cycles between two test procedures, emission factors were normalized to the BJBC. Normalized emission factor of PM_1 mass was 0.082 g/km under low load mass condition over the BJBC. By contrast, it increased by 34 % to 0.110 g/km under high load mass condition.

Measured emission factors of PM_1 number are 3.71×10^{13} and 4.58×10^{13} #/km under the low and high load conditions, respectively, representing an increase of

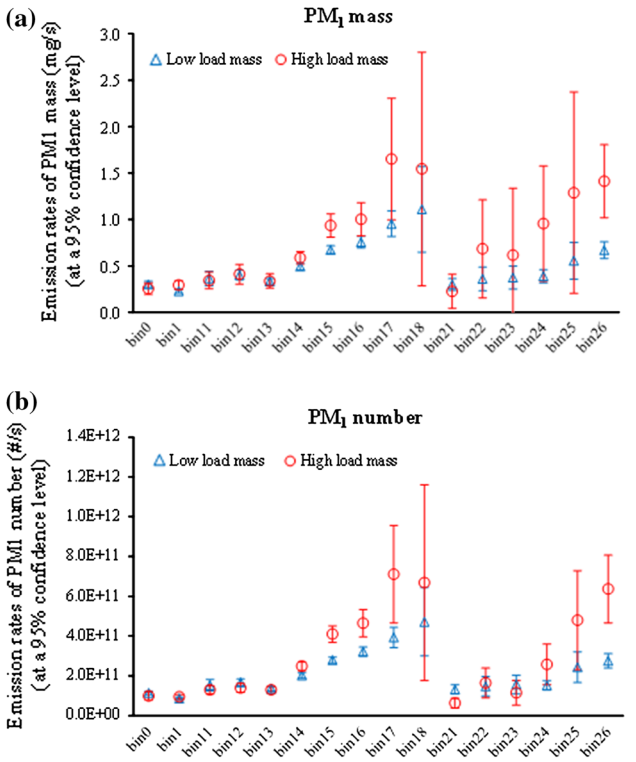

Fig. 5 Average emission rates of PM_1 mass and number for each on-road driving mode

23 %. Figure 5 also presents average emission rates of PM_1 number for each on-road driving mode under both low and high load conditions. They present very similar trends to emission rates of particle mass; emission rates of particle number also generally increased with VSP. For those on-road driving modes with VSP higher than 0 kW/t, average emission rates of particle number were significantly higher under the high load condition, relative to those under the low load condition. In addition, normalized emission factors of PM_1 number were 3.33×10^{13} and 4.28×10^{13} #/km, increased by 28 %, under the BJBC. Our results are also comparable to previously measured results of Euro IV diesel buses in Beijing with an ELPI (Liu et al. 2011).

Size distribution of PM_1 mass and number concentration

Figure 6 presents overall size distributions of PM_1 mass and number concentration under low and high load conditions, respectively. For particle mass emissions, bimodal distributions were observed under low load conditions, with a major peak situated in the fourth channel of ELPI corresponding to the median diameter 173 nm and another minor peak in the sixth channel around 400 nm. However, under high load condition, it is worth noting that the mass share of exhaust particles situated in the eighth channel with the median diameter around 1 μm significantly increased, even higher than those situated in the

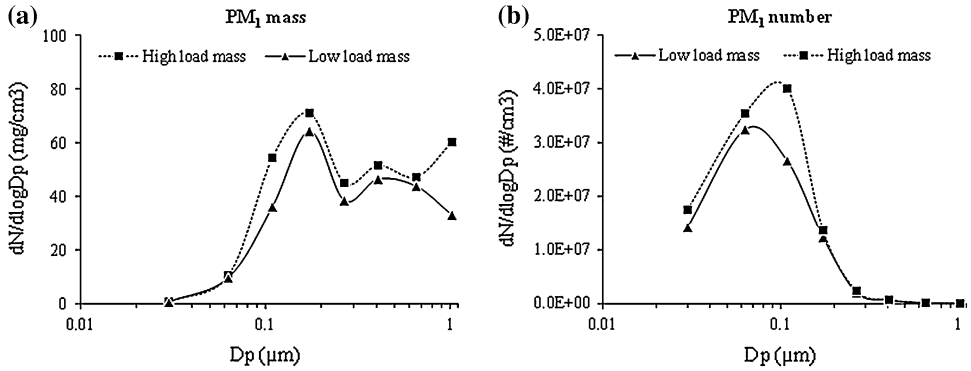

Fig. 6 Size distribution of overall PM_1 mass and number concentration

sixth channel with diameters around 400 nm. For particle number emissions, they complied with typical unimodal distributions under both low and high load conditions, with obvious peaks situated in the second and third channels of ELPI corresponding to the median diameters 63 and 109 nm, respectively. A previous study also observed that most of the particle numbers detected by the ELPI (i.e., median diameter higher than 30 nm) occurred in the accumulation mode with a size range 50–200 nm (Liu et al. 2011). They were typical accumulation particles composed primarily of carbonaceous agglomerates (Lu et al. 2012; Kittelson et al. 2006). Size-resolved concentration of PM_1 mass is not consistent with that of PM_1 number. Nanometer fractions of PM with aerodynamic diameter <200 nm make significant contributions to particle number concentration but play a minor role in particle mass concentration. Since more evidences indicate that nanometer-sized PM is more associated with mortality compared to the fraction with larger size (Kroll et al. 2013), particle number might be a more reasonable indictor of health impacts compared to particle mass. It should be pointed out that the exhaust particles with a median diameter smaller than 30 nm are not observed due to the measurable size range of this ELPI unit (i.e., median diameter from 30 nm to ~1 μm). Those particle profiles with smaller size (e.g., median diameter lower than 30 nm) could be measured by using more advanced measurement instruments (e.g., the Dekati ELPI + with measurable particle median diameter from 6 nm to 10 μm) in the future.

We further explore the impacts of engine-operating conditions on particle size distribution. Size distribution of particle mass and particle number under two load conditions is presented in Figs. 7 and 8, respectively. For particle mass emissions, we can clearly find that size distributions of particles for all engine-operating modes (i.e., BIN 01–06) present bimodal forms under the low load condition, with two clear peaks around 173 and 400 nm, respectively. When load mass increased to 2.0 t, particle mass concentration of BIN 05 and BIN 06 around two peak diameters (i.e., 170 and 400 nm) significantly increased. In addition, for engine-operating modes from BIN 01 to BIN 04, particle mass concentration with aerodynamic diameter around 1 μm became substantially larger under high load conditions, even higher than those with an aerodynamic diameter around 400 nm. In terms of particle number emissions, we can observe obvious unimodal distributions for all engine-operating modes under both low and high load conditions, with peaks situated in the second and third channels of ELPI, respectively, corresponding to the median diameters 63 and 109 nm. It is notable that an abnormal trend of particle mass distribution is observed under high load mass condition for BIN 04 (Fig. 7b). This may be associated with the very low time share (~2 %) of BIN 04 (see Fig. 4), which represents operating conditions of moderately high engine load rate and low engine speed. More measurement data would be required to address this observation in the future.

Table 3 also presents impacts of load mass on particle size distribution indicated by the geometric mean diameter (GMD). For example, GMD for each engine load is higher under the high load mass condition, especially under BIN 06. This is because the increase in load mass would probably result in a higher portion of unmixed fuel and air and further increase exhaust PM concentration (Chuepeng et al. 2011; Tsolakis 2006; Zhu et al. 2011). Meanwhile, coagulation rate is also increased with the PM concentration, which could lead to more particles with larger size (Nabi et al. 2012).

Conclusion

On-road emissions of PM_1 were tested from a Euro IV diesel bus in Beijing under low and high load mass conditions. PM_1 mass and number emissions were recorded second by second using an ELPI. Twenty-two on-road driving modes were constructed using VSP and vehicle speed to relate instantaneous emission rate with real-world driving conditions. Furthermore, six engine-operating modes defined by OBD recorded data regarding engine load rate and engine speed were also developed to explore the impacts of engine load on PM_1 emission characteristics. Our study could provide needed data of on-road PM emission profiles for HDDVs (e.g., particle mass, particle number, and size distribution) as well as the impacts of real-world operating conditions (engine conditions and loading mass) for further emission control in urban areas of China.

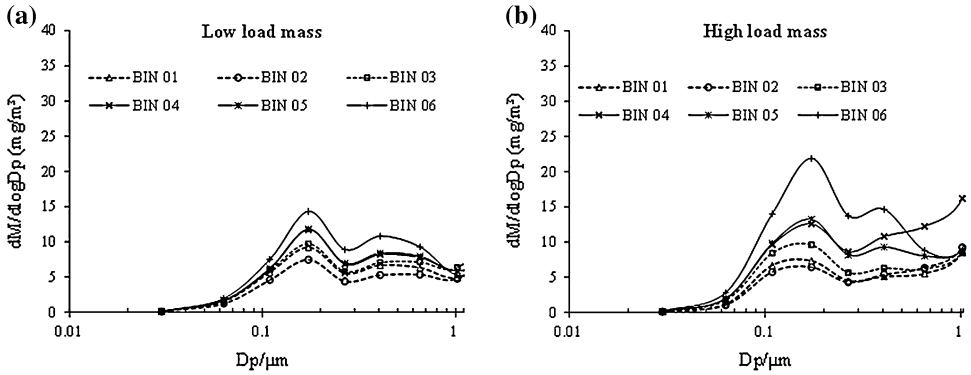

Fig. 7 Size-resolved PM_1 mass concentration by engine-operating mode

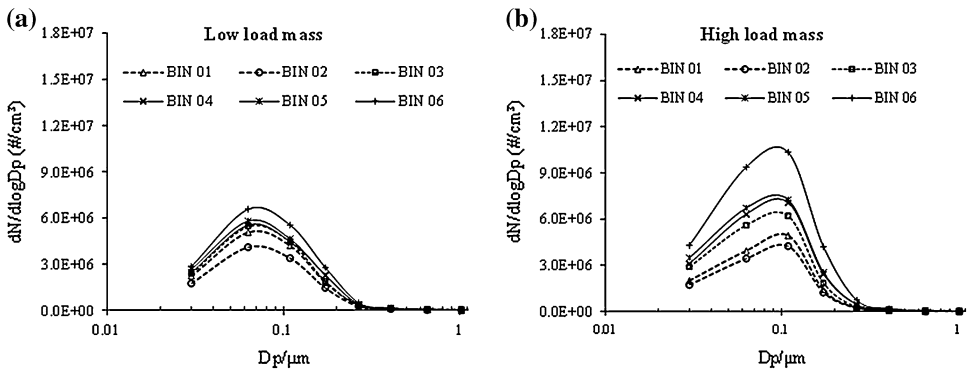

Fig. 8 Size-resolved PM_1 number concentration by engine-operating mode

Table 3 Geometric mean diameters of PM_1 of each engine-operating mode

Load mass	Geometric mean diameter (nm, 95 % CL)					
	BIN 01	BIN 02	BIN 03	BIN 04	BIN 05	BIN 06
Low load mass	73.2 ± 0.2	72.6 ± 0.2	72.4 ± 0.3	72.1 ± 0.5	72.5 ± 0.1	73.7 ± 0.3
High load mass	74.1 ± 0.2	73.7 ± 0.2	72.5 ± 0.3	74.7 ± 0.8	73.4 ± 0.4	75.7 ± 0.6

Emission rates of PM_1 mass and number generally increased with VSP for those on-road driving modes with VSP higher than 0 kW/t, similar to the trends of gaseous pollutants. Higher load mass would increase both particle mass and number emissions. Measured PM_1 mass emission factors were 0.147 and 0.185 g/km under low and high load mass conditions, respectively. In terms of PM_1 number emission factor, they were 3.71×10^{13} and 4.58×10^{13} #/km, representing an increase of 23 % for the higher load mass.

Typical unimodal distributions of size-resolved PM_1 number concentration were observed under both low and high load mass conditions. Nanometer fractions of PM_1 with diameter <200 nm make significant contributions to particle number concentration. For size-resolved PM_1 mass concentration, they presented bimodal distributions under low and high load mass conditions. Furthermore, we also identified impacts of load mass on size-resolved concentration of PM mass and number. For example, under low load mass condition, an obvious peak of PM number concentration was observed around 63 nm situated in the second channel of ELPI. By contrast, peak concentration of PM number was increased under high load mass condition, situated in the third channel of ELPI corresponding to the median diameter 109 nm.

Acknowledgments This work was supported by the National Natural Science Foundation of China (No. 51322804 and No. 51378285), the National High Technology Research and Development Program (No. 013AA065303), special fund of State Key Joint Laboratory of Environment Simulation and Pollution Control (12L05ESPC), the Chinese Academy of Engineering (No. 2013-06-ZD-001), and the Program for New Century Excellent Talents in University (NCET-13-0332). The authors also thank Mr. Chuck Freed, formerly of US EPA for his helpful advice to improve this paper. The contents of this paper are solely the responsibility of the authors and do not necessarily represent official views of the sponsors.

References

Benbrahim-Tallaa L, Baan RA, Grosse Y, Lauby-Secretan B, Ghissassi FE, Bouvard V, Guha N, Loomis D, Straif K (2012)

Carcinogenicity of diesel-engine and gasoline-engine exhausts and some nitroarenes. Lancet Oncol 13(7):663–664
Chuepeng S, Xu H, Tsolakis A, Wyszynski M, Price P (2011) Particulate matter size distribution in the exhaust gas of a modern diesel engine fuelled with a biodiesel blend. Biomass Bioenergy 35:4280–4289
Du X, Wu Y, Fu L, Wang S, Zhang S, Hao J (2012) Intake fraction of $PM_{2.5}$ and NO_X from vehicle emissions in Beijing based on personal exposure data. Atmos Environ 57:233–243
Giechaskiel B, Mamakos A, Andersson J, Dilara P, Martini G, Schindler W, Bergmann A (2012) Measurement of automotive nonvolatile particle number emissions within the European legislative framework: a review. Aerosol Sci Technol 46:719–749
Grieshop AP, Lipsky EM, Pekney NJ, Takahama S, Robinson AL (2006) Fine particle emission factors from vehicles in a highway tunnel: effects of fleet composition and season. Atmos Environ 40(Supplement 2):287–298
Hao J, Wu Y, Fu L, He D, He K (2001) Source contributions to ambient concentrations of CO and NO_X in the urban area of Beijing. J Environ Sci Health A36(2):215–228
Kho FWL, Law PL, Ibrahim SH, Sentian J (2007) Carbon monoxide levels along roadway. Int J Environ Sci Technol 4(1):27–34
Kittelson DB, Watts WF, Johnson JP (2006) On-road and laboratory evaluation of combustion aerosols-Part1: summary of diesel engine results. J Aerosol Sci 37:913–930
Koupal J, Nam E, Giannelli B (2004) The MOVES approach to modal emission modeling. In: 14th CRC On-road Vehicle Emissions Workshop, San Diego
Kroll A, Gietl JK, Wiesmüller GA, Günsel A, Wohlleben W, Schnekenburger J, Klemm O (2013) In vitro toxicology of ambient particulate matter: correlation of cellular effects with particle size and components. Environ Toxicol 28(2):76–86
Kuhns HD, Mazzoleni C, Moosmüller H, Nikolic D, Keislar RE, Barber PW, Li Z, Etyemezian V, Watson JG (2004) Remote sensing of PM, NO, CO and HC emission factors for on-road gasoline and diesel engine vehicles in Las Vegas, NV. Sci Total Environ 322(1–3):123–137
Lähde T, Rönkkö T, Happonen M, Söderström C, Virtanen A, Solla A, Kytö M, Rothe D, Jorma K (2011) Effect of fuel injection pressure on a heavy-duty diesel engine nonvolatile particle emission. Environ Sci Technol 45:2504–2509
Liu Z, Ge Y, Johnson KC, Shah AN, Tan J, Wang C, Yu L (2011) Real-world operation conditions and on-road emissions of Beijing diesel buses measured by using portable emission measurement system and electric low-pressure impactor. Sci Total Environ 409(8):1476–1480
Lu T, Cheung CS, Huang Z (2012) Effects of engine operating conditions on the size and nanostructure of diesel particles. J Aerosol Sci 47:27–38
Malakootian M, Yaghmaeian K (2004) Investigation of carbon monoxide in heavy traffic intersections of municipal districts. Int J Environ Sci Technol 1(3):227–231
Maricq MM (2007) Chemical characterization of particulate emissions from diesel engines: a review. J Aerosol Sci 38:1079–1118
Maricq MM, Xu N, Chase RE (2006) Measuring particulate mass emissions with the electrical low pressure impactor. Aerosol Sci Technol 40:68–79
Mazzarella G, Esposito V, Bianco A, Ferraraccio F, Prati MV, Lucariello A, Manente L, Mezzogiorno A, Luca A (2012) Inflammatory effects on human lung epithelial cells after exposure to diesel exhaust micron sub particles ($PM_{1.0}$) and pollen allergens. Environ Pollut 161:64–69
Nabi MN, Brown RJ, Ristovski Z, Hustad JE (2012) A comparative study of the number and mass of fine particles emitted with diesel fuel and marine gas oil (MGO). Atmos Environ 57:22–28
Oberdorster G, Sharp Z, Atudorei V, Elder A, Gelein R, Kreyling W, Cox C (2004) Translocation of inhaled ultrafine particles to the brain. Inhal Toxicol 16:437–445
Pope CA (2000) Review: epidemiological basis for particulate air pollution health standards. Aerosol Sci Technol 32:4–14
Scheepers PT, Vermeulen RC (2012) Diesel engine exhaust classified as a human lung carcinogen. How will this affect occupational exposures? Occup Environ Med 69:691–693
Somers CM, McCarry BE, Malek F, Quinn JS (2004) Reduction of particulate air pollution lowers the risk of heritable mutations in mice. Science 304:1008–1010
Song S, Wu Y, Jiang J, Yang L, Cheng Y, Hao J (2012) Chemical characteristics of size-resolved $PM_{2.5}$ at a roadside environment in Beijing, China. Environ Pollut 161:215–221
Song S, Wu Y, Xu J, Ohara T, Hasegawa S, Li J, Yang L, Hao J (2013) Black carbon at a roadside site in Beijing: temporal variations and relationships with carbon monoxide and particle number size distribution. Atmos Environ 77:213–221
Tang UW, Wang Z (2006) Determining gaseous emission factors and driver's particle exposures during traffic congestion by vehicle-following measurement techniques. J Air Waste Manag Assoc 56:1532–1539
Tsolakis A (2006) Effects on particle size distribution from the diesel engine operating on RME-biodiesel with EGR. Energy Fuels 20:1418–1424
Ushakov S, Valland H, Nielsen JB, Hennie E (2013) Particle size distributions from heavy-duty diesel engine operated on low-sulfur marine fuel. Fuel Process Technol 106:350–358
Wang X, Westerdahl D, Wu Y, Pan X, Zhang KM (2011) On-road emission factor distributions of individual diesel vehicles in and around Beijing, China. Atmos Environ 45(2):503–513
Wang X, Westerdahl D, Hu J, Wu Y, Yin H, Pan X, Zhang KM (2012) On-road diesel vehicle emission factors for nitrogen oxides and black carbon in two Chinese cities. Atmos Environ 46:45–55
Wang Z, Wu Y, Zhou Y, Li Z, Wang Y, Zhang S, Hao J (2013) Real-world emissions of gasoline passenger cars in Macao and their correlation with driving conditions. Int J Environ Sci Technol. doi:10.1007/s13762-013-0276-2
Wu Y, Wang R, Zhou Y, Lin B, Fu L, He K, Hao J (2011) On-road vehicle emission control in Beijing: past, present and future. Environ Sci Technol 45(1):147–153
Wu Y, Yang Z, Lin B, Liu H, Wang R, Zhou B, Hao J (2012a) Energy consumption and CO_2 emission impacts of vehicle electrification in three developed regions of China. Energy Policy 48:537–550
Wu Y, Zhang S, Li M, Ge Y, Shu J, Zhou Y, Xu Y, Hu J, Liu H, Fu L, He K, Hao J (2012b) The challenge to NO_X emission control for heavy-duty diesel vehicles in China. Atmos Chem Phys 12:9365–9379
Wu Y, Yang L, Zheng X, Zhang S, Song S, Li J, Hao J (2014) Characterization and source apportionment of particulate PAHs in the roadside environment in Beijing. Sci Total Environ 470–471:76–83
Zervas E, Dorlhene P, Forti L, Perrin C, Momique JC, Monier R, Ing H, Lopez B (2006) Exhaust gas particle mass estimation using an electrical low pressure impactor. Energy Fuels 20:498–503
Zhang S, Wu Y, Liu H, Wu X, Zhou Y, Yao Z, Fu L, He K, Hao J (2013) Historical evaluation of vehicle emission control in Guangzhou based on a multi-year emission inventory. Atmos Environ 76:32–42
Zhang S, Wu Y, Liu H, Huang R, Yang L, Li Z, Fu L, Hao J (2014) Real-world fuel consumption and CO_2 emissions of urban public buses in Beijing. Appl Energy 113:1645–1655
Zhou Y, Wu Y, Yang L, Fu L, He K, Wang S, Hao J, Chen J, Li C (2010) The impact of transportation control measures on emission reductions during the 2008 Olympic Games in Beijing, China. Atmos Environ 44(3):285–293
Zhu R, Cheung CS, Huang Z, Wang X (2011) Experimental investigation on particulate emissions of a direct injection diesel engine fueled with diesel–diethyl adipate blends. J Aerosol Sci 42:264–276